www.elsevier.com/locate/jobe

Investigation of the relationship between the allowable transparent area, thermal mass and air change rate in buildings

Imre Csáky, Ferenc Kalmár

PII: S2352-7102(17)30084-0
DOI: http://dx.doi.org/10.1016/j.jobe.2017.05.002
Reference: JOBE259

To appear in: *Journal of Building Engineering*

Received date: 10 February 2017
Revised date: 2 May 2017
Accepted date: 2 May 2017

Cite this article as: Imre Csáky and Ferenc Kalmár, Investigation of th relationship between the allowable transparent area, thermal mass and air chang rate in buildings, *Journal of Building Engineering* http://dx.doi.org/10.1016/j.jobe.2017.05.002

Investigation of the relationship between the allowable transparent area, thermal mass and air change rate in buildings

Imre Csáky, Ferenc Kalmár*

University of Debrecen, Faculty of Engineering, 4028 Debrecen, Ótemető u. 2-4, Hungary

imrecsaky@eng.unideb.hu

fkalmar@eng.unideb.hu

*Corresponding author. Tel: +36 52 415155; Fax: +36 52 418643

Abstract

In recent years, because of the high heat loads during the summer period and increased comfort needs of occupants, the energy used for the air conditioning of buildings has increased in most European countries. Choosing circumspectly the building materials and the transparent areas on the facades, proper indoor thermal conditions can be assured without cooling the fresh air. However, in this case the ventilated air flow has to be controlled properly. The aim of our research was to investigate the effects of thermal mass and air change rate on the allowable transparent area for different orientations of facades. Measurements were performed in a special rotating laboratory to determine the relation between thermal mass, incident radiation and indoor temperature. The incident solar radiation was determined for vertical surfaces using the measured global radiation data from 2009–2013. Measurements were carried out to determine the effect of stored heat on the internal air temperature excluding the effect of air change rate and solar radiation. Using the methodology given by standard EN ISO 13790, the allowable transparent area was determined assuming different building materials and air change rates. Based on calculations effectuated on 688 building models, it was proved that there is a linear relation between allowable transparent area and air change rate.

Keywords

air change rate, building materials, solar gains, thermal comfort, thermal mass

1. Introduction

Energy savings is one of the key priorities in the building sector. According to Directive 2010/31/EU of the European Parliament, the Council Member States shall ensure that by 31 December 2020, all new buildings are nearly zero-energy buildings [1]. Because of the strict national requirements regarding the maximum admissible value of overall heat transfer coefficients, the envelopes of buildings are increasingly insulated and airtight. Nevertheless, people need fresh air and daylight. Both are crucial to obtain maximal work efficiency and preconditioning of an appropriate comfort feeling in closed spaces. Newly constructed buildings usually have large, transparent areas that provide great views and psychologically positive impulses for occupants, allowing natural light to enter the closed spaces. Unfortunately, during the summer periods, these large, transparent areas can lead to huge heat loads, and proper thermal comfort can be ensured in many cases only by using air conditioning systems. This is accentuated by the fact that the number and amplitude of heat waves during summer have increased in recent decades [2]. According to Schar et al. the drought conditions amplify local temperature anomalies, [3]. During droughts the net balance of solar and infrared radiation is almost entirely balanced by local heating, while evapotranspiration is suppressed owing to the lack of soil moisture, [3]. The impact of soil moisture anomalies on the precipitation was analyzed by Koster et al. [4]. There is a strong relationship between the soil moisture, cloudiness, radiation and temperature, [5]. Beniston et al. forecasted that the regions such as France and Hungary, for example, may experience as many days/year above 30°C in the future as are currently experienced in Spain and Sicily, [6]. The energy used for air conditioning in the summer period can be reduced by the proper selection of glazing elements and accurate design of shading. Furthermore, the amplitude of indoor air temperature variation can be reduced if the thermal mass of the closed spaces is suitably calculated, adequately located and distributed such that the ventilation system is used in an intelligent way.

Pearlmutter and Meir demonstrated that in summer, tenants of lightweight buildings in the desert will either be faced with overheated conditions, or consume considerable amounts of energy to cool the buildings down to comfort limits, [7]. Large transparent areas can lead to extreme indoor temperatures even in temperate continental climate conditions, [8]. Jenkins et al proposed an algorithm to predict overheating in buildings using probabilistic climate projections, [9]. Overheating Al Sanea et al. analyzed in detail the energy saving potential of thermal mass [10]. They calculated the optimal thickness of thermal mass taking into account the total and peak transmission loads, time lag, decrement factor, and dynamic under steady periodic conditions using the climatic data of Riyadh. Cheng et al demonstrated that choosing properly the color and the thermal mass of a building envelope the indoor temperatures can be drastically reduced even in hot humid climates, [11]. Choosing properly the thermal mass the required indoor thermal comfort parameters can be achieved without mechanical ventilation of buildings. There is a significant impact of multiple factors of climate, building properties, occupancy and operation profiles on the performance of natural ventilation. Yao et al. investigated the natural ventilation cooling potential of office buildings in the five climate zones in China using the Thermal Resistance Ventilation (TRV) model, which is a simplified, coupled, thermal and airflow model, [12]. Zhou et al. developed a simple tool to estimate the indoor air temperature for certain external and internal thermal mass and to determine the internal thermal mass needed to maintain required indoor air temperature for certain external wall for naturally ventilated building, [13]. La Roche and Milne developed an intelligent ventilation controller that can manage airflow according to cooling the needs in a building and the resources in the environment, [14]. They presented controller strategy that optimizes

cooling with outdoor air. Schulze and Eicker analyzed the energy saving by controlled natural ventilation in three locations (Stuttgart, Turin and Istanbul).

According to Balaras, a 5–10 cm wall thickness is suitable for heat absorption, storage and release on a daily basis. Thicker walls, up to 25 cm, may provide longer periods of thermal storage [15]. Yang and Li demonstrated that an increased time constant of more than 400 h can effectively reduce the cooling load by more than 60% [16]. The efficiency of the thermal mass can be increased by coupling it with natural night ventilation [17]. Shaviv et al. demonstrated that the exact reduction in the maximum indoor temperature depends on the amount of thermal mass, the rate of night ventilation, and the temperature swing of the site between day and night [18]. Lee and Braun suggested a demand-limiting control methodology of the thermal mass. Their model-based, demand-limiting strategy was implemented at a site, resulting in a 30% reduction in peak cooling load compared with conventional control for a 5-h afternoon demand-limiting period [19]. Braun et al. developed a tool that allows the evaluation of the performance of building thermal mass control strategies [20]. The energy savings depend upon utility incentives, building construction, climate, and the type of air conditioning system. Zheng et al. attempted to find the optimal specific heat of building materials and the optimal natural ventilation rate to minimize the energy use of buildings [21].

Based on measurements carried out in the PASSOL laboratory and Building Physics laboratory of University of Debrecen and the aforementioned findings, we developed a methodology that allows the maximum admissible glazed area of a closed space to be determined depending on the orientation of the facade and the thermal mass. Usually, in practice, the building materials are chosen first and the thermal mass of a building or room is a given parameter depending on the geometry of a closed spaces. The thermal mass rarely is adjusted in function of the transparent area. In present study, we tried to determine the allowable transparent area for a room depending on the thermal mass and air change rate assuming widely used building materials.

2. Objectives and hypothesis

There are numerous simulations or measurements carried out in order to find the optimal thermal mass in order to minimize the cooling energy need. We consider the thermal mass a given physical parameter of the room and the main goal was to determine the allowable transparent area (depending on the orientation, thermal mass and air change rate) in order to keep the operative indoor temperature under the maximum admitted value for a “B” comfort category (26 °C). Our hypothesis was that the operative temperature can be kept under 26 °C without cooling systems even in case of buildings built from traditional building materials.

3. Measurements in PASSOL laboratory

At the Department of Building Services and Building Engineering at the University of Debrecen, a special rotating room called PASSOL was built, [22]. The panels are laid on a special mechanism that permits the rotation of the whole room around its own axis (Figure 1).

Figure 1. Test room.

Considering the shading of the surrounding objects for May, June, July and August, the indoor temperature variation was analyzed, using the methodology presented by European Standard EN ISO 13790 [23] and the global solar radiation and hourly dry bulb temperature records from 2009 to 2013, provided by Agro-Meteorological Observatory Debrecen. The differences between the calculated and measured temperature values were negligible [24]. The next step of our research was to investigate the effect of thermal mass on the indoor temperature variation. On the floor of the test box, a sand layer was laid down. The density of the sand was ρ= 1600 [kg/m^3], the thermal conductivity was λ= 0.58 [W/mK], and the specific heat was c= 840 [J/kgK]. The thickness of the sand layer was increased weekly—5.0, 10.0, 15.0 and finally 20.0 cm—and the effect of different thicknesses on the indoor temperature was analyzed.

In Figure 2, the incident radiation on the south-orientated vertical surfaces is presented for two consecutive days, when the thickness of the sand layer was 5.0 cm and 15.0 cm, respectively. It can be observed that the solar radiation was similar in these two situations.

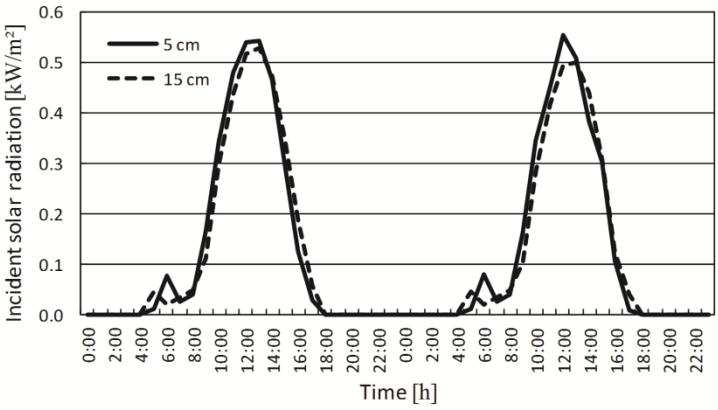

Figure 2. Solar radiation on south-oriented vertical surface.

The variation of outdoor temperature for the analyzed days is presented in Figure 3.

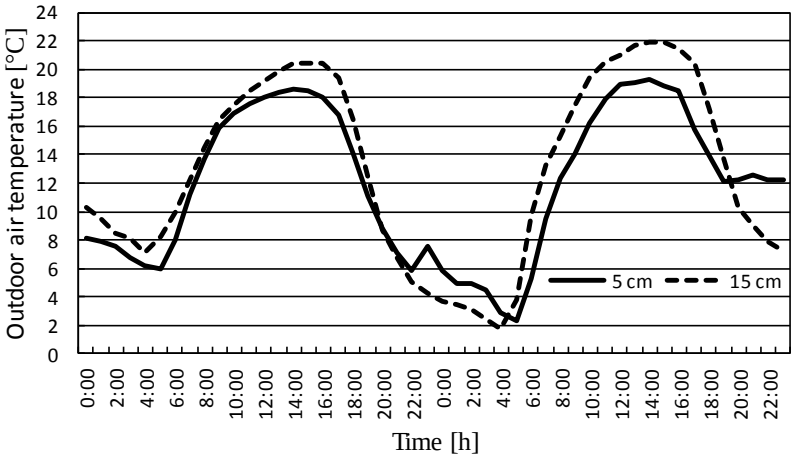

Figure 3. Outdoor temperature variation for analyzed days.

It can be observed that in the case of the 5.0 cm thick thermal mass layer, we had a slightly colder day. Nevertheless, the indoor air temperature, measured at different heights (0.1 m, 1.1 m and 1.7 m), presented lower values in the case of the 15.0 cm thick thermal mass (Figure 4).

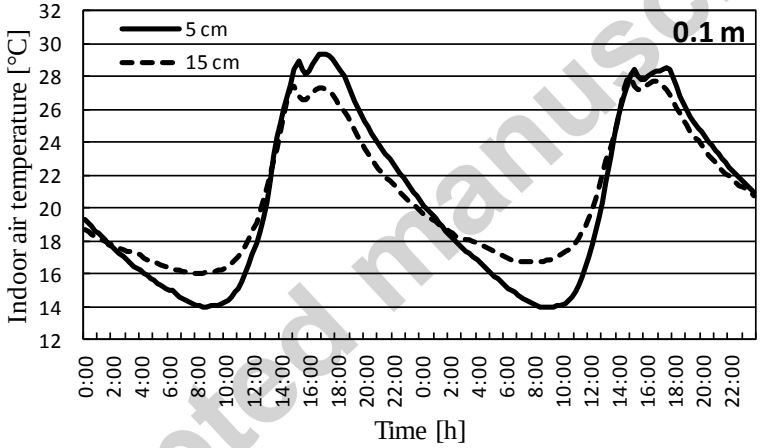

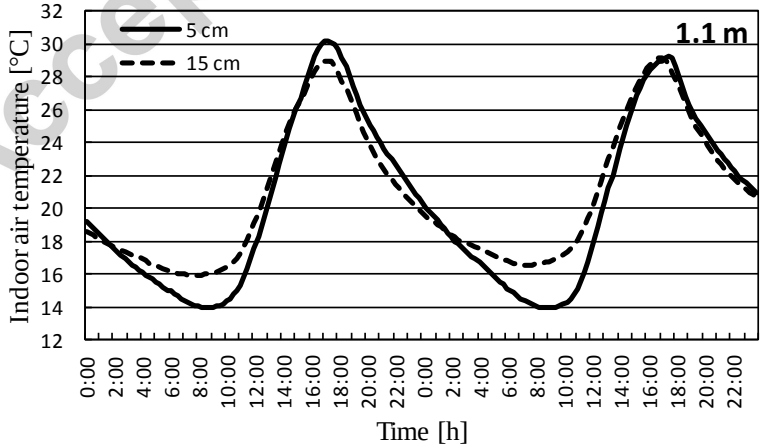

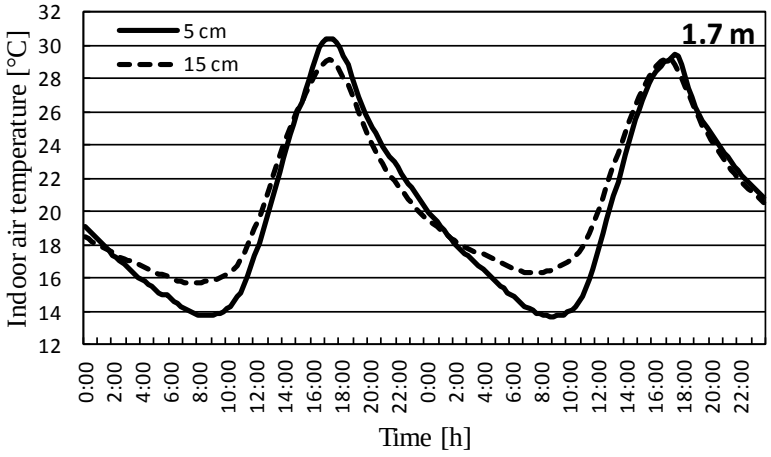

Figure 4. Measured indoor air temperature at different heights.

Using the methodology given by European Standard EN ISO 13790 [23] and assuming similar incident radiation on the horizontal and vertical surfaces, the variation in the indoor air temperature was determined in the middle of the room for different thicknesses of the thermal mass. The results are presented in Figure 5. It can be observed that by increasing the thickness of the thermal mass, the indoor temperature can be reduced considerably. However, the first 5.0 cm has the highest effect on the amplitude of the indoor air temperature (a reduction of approximately 8.0 K). For thicknesses of thermal mass of 5.0 cm and 10.0 cm, there is a difference between the amplitudes of indoor air temperature of approximately 1.8 K. By increasing the thermal mass thickness from 10.0 cm to 15.0 cm, the amplitude of the indoor air temperature decreases by approximately 0.2 K. Further increasing the thermal mass thickness to 20.0 cm results in no difference between the amplitudes of indoor air temperatures.

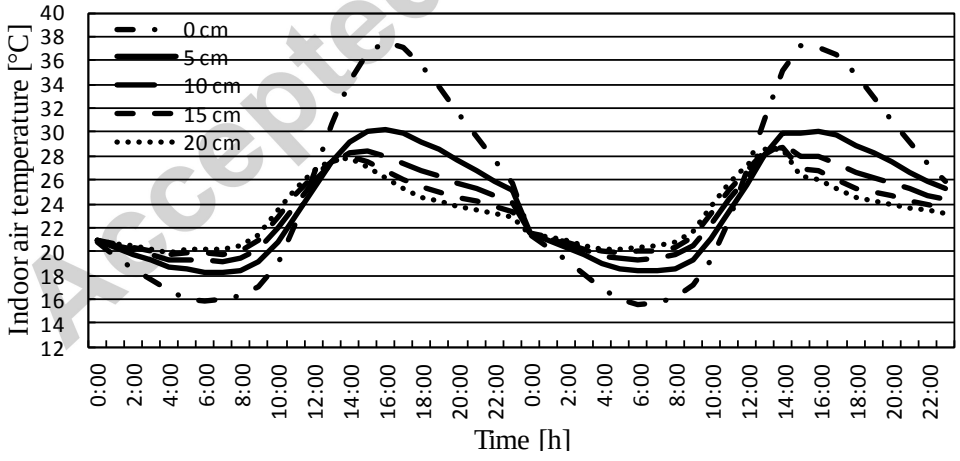

Figure 5. Variation of indoor air temperature for different thicknesses of the thermal mass.

4. Measurements in Building Physics laboratory

A climatic chamber is available in the Building Physics laboratory at the Department of Building Services and Building Engineering at the University of Debrecen. This chamber is suitable for testing the heat storage of different building materials while avoiding the effects of solar radiation and air change rate. The chamber is surrounded with 0.3 m thick EPS 200 and divided into two rooms (2.2×3.4×2.4 m^2 each) by a 0.5 m thick EPS 200 insulating system (Figure 6).

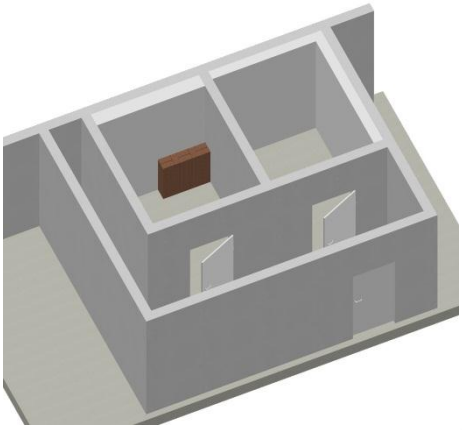

Figure 6. Scheme of the Building Physics laboratory

One of the test rooms is practically a climatic chamber because its temperature can be set between 250 K and 298 K. The other room can only be warmed to 298 K. In the climatic chamber, a series of air temperature measurements were carried out, changing the heat capacity of the room. Measurements were also performed without any supplementary material in the test room (light structure). The thermal mass of the room was changed by placing different building materials in the room, which covered 1 m^2 of the wall of the test room (Figure 6): solid brick (SB), autoclaved aerated concrete (AAC), and brick with vertical holes (BVH). The physical properties of these building materials are presented in table 1.

Table 1. Physical properties of building materials.

Building material	Density, [kg/m^3]	Thermal conductivity, [W/mK]	Specific heat, [J/kgK]	Total mass, [kg]
SB	1730	0.72	880	415
BVH	750	0.17	880	224
AAC	600	0.138	1000	180

The aim of the measurements was to investigate the effect of thermal mass and different building materials on the internal temperature variation after switching on/off the heating or cooling system. In the first series of measurements, the air temperature in the room

was kept constant (20 °C) for 24 h, then the air was heated to 24 °C. When the air temperature reached 24 °C, the heating device was switched off. The indoor air temperature was registered minutely using a KIMO KH100 data logger for 4 h. Taking as a reference t_r=20 °C, the variations of the difference between the registered indoor air temperature and the reference temperature $\Delta t = t_i - t_r$ are presented in Figure 7.

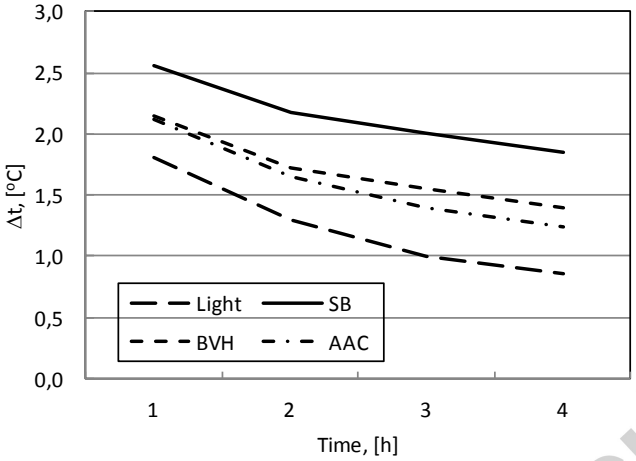

Figure 7. Variation of Δ*t* after heating to 24 °C.

It can be observed that in the case of a light structure (practically no thermal mass), the air temperature decreased rapidly to 20 °C. In the case of SB, BVH and AAC, because of the accumulated heat, the air temperature decreased slowly. With low thermal conductivity values in the case of AAC and BVH, the stored heat is lower; consequently, the air temperature is closer to the reference value.

In the case of the second series of measurements, the air temperature in the room was kept constant (20 °C) for 24 h, then the air was heated to 28 °C. When the air temperature reached 28 °C, the heating device was switched off. The variation Δ*t* is presented in Figure 8 (reference temperature t_r=20 °C).

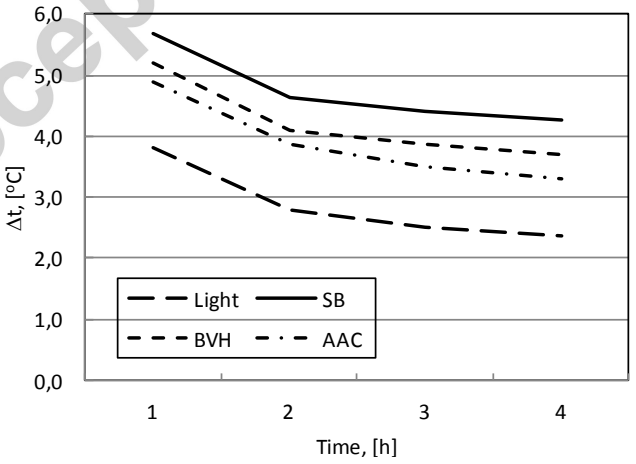

Figure 8. Variation of Δ*t* after heating to 28 °C.

It can be seen that the trend of air temperature variation is similar to the previous case, but the air temperature is higher by approximately 2–3 K if a thermal mass is placed in the room.

In the third case, we maintained the room at 24 °C for 24 h, and then the air in the room was cooled to 20 °C. When the air temperature reached 20 °C, the cooling device was switched off. The variation of Δt is presented in Figure 9 (reference temperature t_r=20 °C).

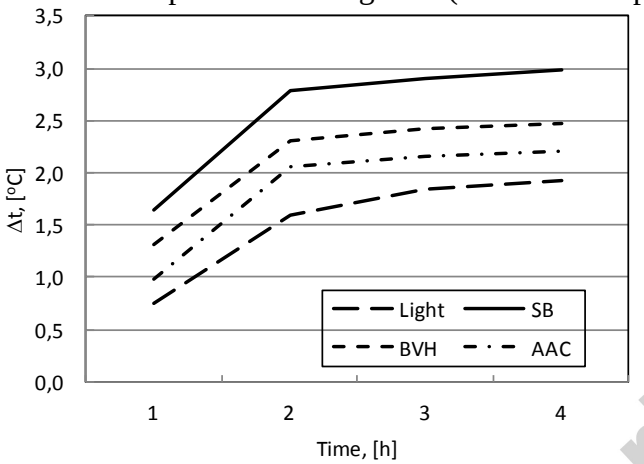

Figure 9. Variation of Δt after cooling from 24 °C.

It can be observed that the air temperature increased after switching off the cooling device. Depending on the stored heat in the thermal mass, after 4 h, the air temperature was between 22 °C and 24 °C. It is interesting that in this case, the effect of the thermal mass is lower compared with previous cases. Furthermore, the highest increase of the air temperature is registered in the first 2 h. Thereafter, the growth of the indoor air temperature is small.

In the fourth case, the room was maintained at 28 °C for 24 h, and then the air in the room was cooled to 20 °C. When the air temperature reached 20 °C, the cooling device was switched off. The variation of Δt is presented in Figure 10 (reference temperature t_r=20 °C).

The trend of the indoor air temperature variation is similar to the previous case, but because of the higher quantity of stored heat, higher temperature values were registered.

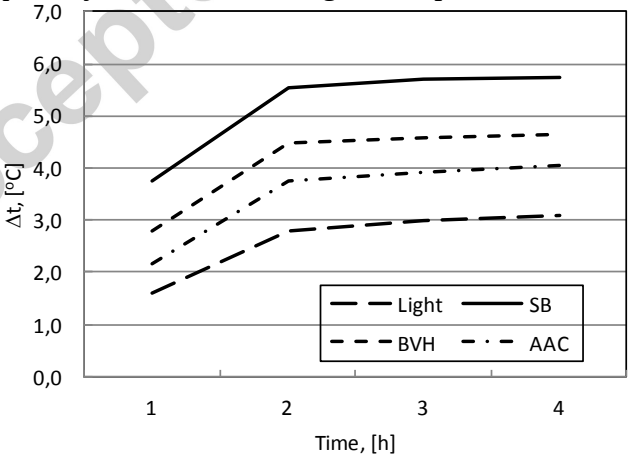

Figure 10. Variation of Δt after cooling from 28 °C.

These experiments have proven that the sudden variation of heat load in a closed space results in different oscillation profiles of indoor air temperatures. The amplitude and

periodicity of oscillation depend mainly on the heat load variation and heat capacity of the closed space. In summer periods, the solar gains are the main source of indoor air temperature variation in buildings. Depending on the orientation of the facades, proper selection of the glazed area and building materials can ensure appropriate thermal comfort in buildings even in summer periods without the use of air conditioning systems.

5. Air change rate, thermal mass and allowable glazed area

Measurements of global solar radiation in Debrecen from 2009–2013 have proved that the highest incident solar radiation is obtained with east and west orientations of the facades. To analyze the relationships among solar gains, air change rate, thermal mass and operative temperature, one of the hottest days of the hottest month (July 2011) in the analyzed period (2009–2013) was chosen as an input for incident solar radiation and outdoor temperatures. The daily mean outdoor temperature on this day was 28.3 °C. The incident solar radiation on vertical surfaces on this day is presented in Figure 11. It can be observed that there is a strong asymmetry between the incident radiation on the E and W facades, [24]. This can be caused by the fact that the cloudiness was different in the morning and in the afternoon. Furthermore, the aerosol content in the air could be higher in the afternoon.

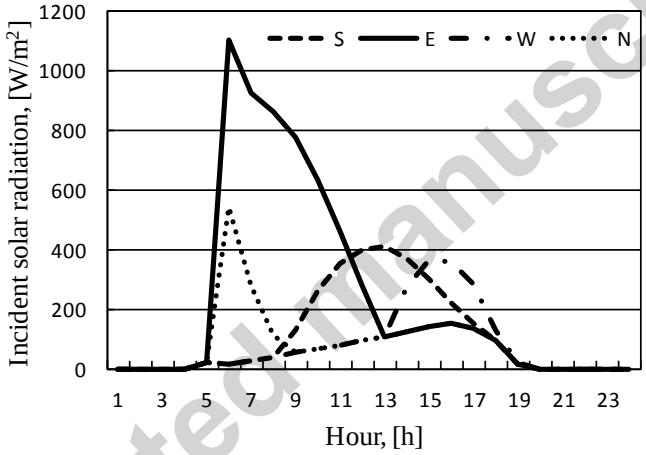

Figure 11. Incident solar radiation on vertical surfaces (input data).

According to the recommendations of Standard EN 15251, in the case of mechanically conditioned buildings for comfort (category II), the operative temperature should be kept between 23 °C and 26 °C [25]. In countries with temperate climates, during summer heatwaves, the operative temperature in buildings without air conditioning systems can hardly be reduced below 24 °C, even if night ventilation is used efficiently. The aim of our further research was to determine the allowable glazed area to maintain the operative temperature between 24 °C and 26 °C, depending on the orientation of the transparent area, building materials, and air change rate.

The calculation method uses the RC network of the heat flows, given by EN ISO 13790:2008..

In the following, the results of a case study are presented. The geometrical characteristics of the analyzed room are: 4.0×4.0×2.8 m. The overall heat transfer coefficients of the external building elements are: U_{wall}= 0.226 W/m^{2}K; U_{floor} = 0.209 W/m^{2}K, U_{window}=1.0 W/m^{2}K; $U_{flatroof}$=0.166 W/m^{2}K. All investigated wall materials—concrete (C), solid brick (SN), brick with vertical holes (BVH), autoclaved aerated concrete (AAC) and the roof—are

provided with an external insulation layer. The calculations were performed based on different room positions in the building. The accepted error of the iterative calculations was 10^{-2}.

A steel framed lightweight structure was analyzed with similar overall heat transfer coefficients to the external building elements, but in this case, the upper operative temperature limit of 26 °C could not be maintained, even for rooms without any transparent area on the facades.

For a corner room situated in the attic of the building (3 external building elements) built from solid brick and insulated outside, the allowable transparent area depending on the glazed facade orientation and air change rate is shown in Figure 12.

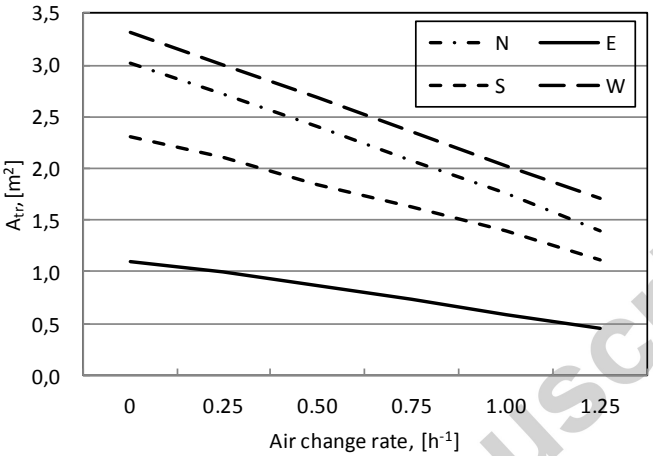

Figure 12. Allowable transparent area for a corner room, depending on the air change rate.

The variation can be considered linear because the coefficient of determination R^2 is higher than 0.995 in each case. The linearity of interrelation between the allowable transparent area and the air change rate was checked for all positions of the room and all orientations (688 cases). Consequently, if the allowable transparent area is known for two air change rate values, then for any other air change rate value, it is valid that

$$A_{tr} = ACH \times tg\alpha \tag{8}$$

where

$$tg\alpha = \left(A_{tr1} - A_{tr2}\right) / \left(ACH_2 - ACH_1\right) \tag{9}$$

Assuming an air change rate of 0.5 h^{-1}, the allowable transparent area for a corner room situated in the attic of the building is illustrated for different wall materials, depending on the orientation of the glazed area in Figure 13.

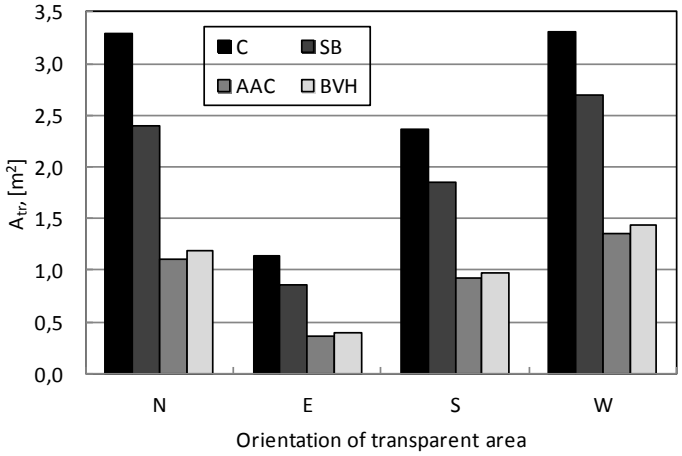

Figure 13. Allowable transparent area depending on the building materials used.

Because the dimensions of the windows in a building are usually similar for each facade and each story, appropriate shading must be ensured to avoid operative temperatures higher than 26 °C. In the analyzed case, the shading percentages are presented in Figure 14 for a three-story building whose walls are solid brick with an air change rate of 0.5 h^{-1} (built-in transparent area 3.0 m^2).

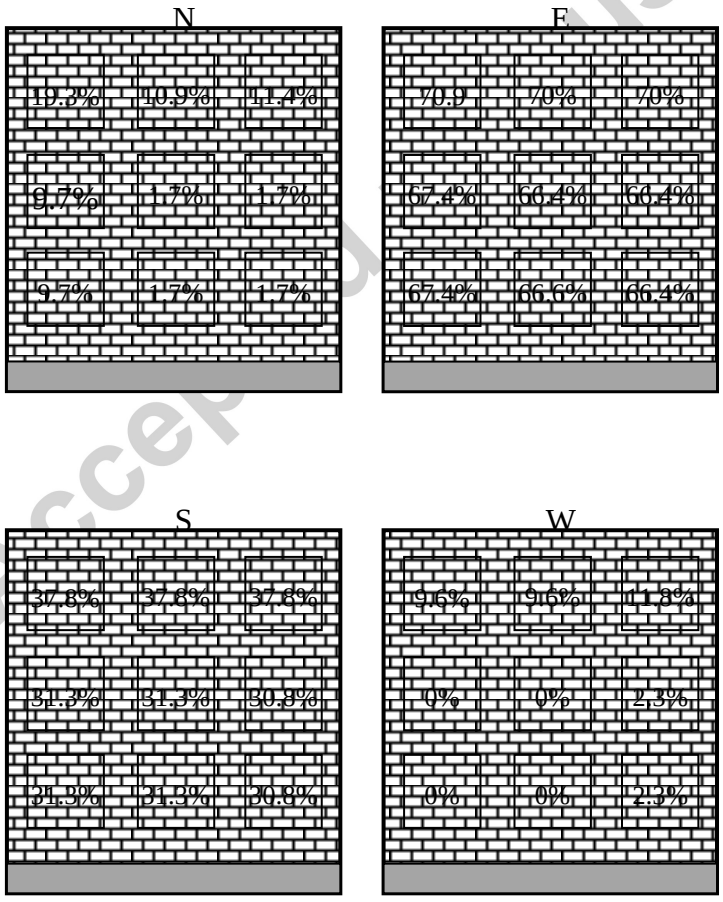

Figure 14. Shading percentages as a function of orientation of the transparent area.

6. Conclusions

Based on the measurements performed in the PASSOL laboratory, the effects of the thermal mass were analyzed for different orientations of the glazed area with no air change rate between the indoor and outdoor environment. It was proven that the amplitude of the indoor air temperature can be reduced by 1.8–8 K, increasing the thermal mass of the room. Furthermore, in the Building Physics laboratory, tests were conducted with no air change and excluding solar radiation measurements to analyze the effects of heat storage on the indoor air temperature with different building materials. It was found that even a 1.0 m^2 area of a conventional building element can change the air temperature in a light structure room by 2 K in the case of a sudden change in the heat load.

Most design methodologies yield similar values for the incident solar radiation on vertical surfaces for east and west orientations. Measurements carried out from 2009 to 2013 proved that in the last five years, the energy yield for east and west orientations shows important asymmetry. In the case of asymmetric days, the incident solar radiation exceeds the solar energy yield of symmetric days. By analyzing one of the hottest days of the last years, it was found that the energy yield on east-oriented vertical surfaces was almost triple that of the energy yield for a west orientation. The asymmetry is caused mainly by the cloudiness and aerosol content of the air. The allowable transparent area (shading percent) was determined for a room situated at different levels and positions of a three-story building. The shading percent is not similar on a façade for rooms with the same geometry. This is caused by the differences between heat gains and losses of rooms situated at different floors of the building (ground floor, intermediate, top) and the room position (corner or middle). The rooms situated in the corner of the buildings have at least two external building elements. Through the façade the heat gains are similar, but the gains are different through adjacent opaque elements because the incident solar radiation depends on the orientation. Analyzing 688 different cases it was found that in addition to the thermal mass, the allowable transparent area is strongly influenced by the air change rate, and this interdependence is linear. This relation was determined assuming that air change rate is constant (mechanical ventilation) and can be used in practice for programming the shading control elements of transparent surfaces.

Acknowledgement

The authors would like to express their gratitude to the Agro-Meteorological Observatory, Debrecen, for providing indispensable meteorological data.

References

[1] EC Directive, (2010), Directive 2010/31/EU of the European Parliament and of the Council of 19 May 2010 on the energy performance of buildings (recast). Official Journal of the European Communities, L 153/13, 18.6.2010, Brussels

[2] Luterbacher J., Dietrich D., Xoplaki E., Grosjean M., Wanner H., (2004), European seasonal and annual temperature variability, trends, and extremes since 1500, Science, 303, 1499.

[3] Schär Ch., Vidale P.L., Lüthi D., Frei Ch. , Haberli Ch., Liniger M.A., Appenzeller Ch., The role of increasing temperature variability in European summer heatwaves, Nature, 427, 332-336.

[4] Koster, R.D., Dirmeyer P.A., Guo Z., Bonan G., Chan E., Cox P., Gordon C.T., Kanae Sh., ,Kowalczyk E., Lawrence D., Ping Liu P.,10 Lu C-H., Malyshev S., McAvaney B., Mitchell K., Mocko D., Oki T., Oleson K., Pitman A., Sud Y.C., Taylor Ch.M., Verseghy D.,Vasic R., Xue Y.,Yamada T., Regions of Strong Coupling Between Soil Moisture and Precipitation, Science, 305, 1138-1140.
[5] Seneviratne S.I., Corti T., Davin E.L., Hirschi M., Jaeger E.B., Lehner I., Orlowsky B., Teuling A.J., Investigating soil moisture–climate interactions in a changing climate: A review, Earth-Science Reviews 99 (2010) 125–161.
[6] Beniston M., Stephenson D.B., Christensen O.B., Ferro Ch., Frei Ch., Goyette S., Halsnaes K., Holt T., Jylhä K., Koffi B., Palutikof J., Schöll R., Semmler T., Woth K., Future extreme events in European climate: an exploration of regional climate model projections, Climatic Change (2007) 81:71–95.
[7] Pearlmutter D., Meir I.A., Assessing the climatic implications of lightweight housing in a peripheral arid region, Building and Environment, 30 (3), (1995), 441-451.
[8] Kalmár F., Summer operative temperatures in free running existing buildings with high glazed ratio of the facadesm Journal of Building Engineering, 6 (2016), 236-242.
[9] Jenkins D.P., Patidar S., Banfill P.F.G., Gibson G.J. Probabilistic climate projections with dynamic building simulation: Predicting overheating in dwellings, Energy and Buildings 43 (2011) 1723–1731.
[10] Al-Sanea S., Zedan M.F., Al-Hussain S.N., Effect of thermal mass on performance of insulated building walls and the concept of energy savings potential, Applied Energy, 89 (2012), 430–442.
[11] Cheng V., Ng E., Givoni B., Effect of envelope colour and thermal mass on indoor temperatures in hot humid climate, Solar Energy 78 (2005) 528–534.
[12] Yao R., Li B., Steemers K., Short A., Assessing the natural ventilation cooling potential of office buildings in different climate zones in China, Renewable Energy 34 (2009) 2697–2705.
[13] Zhou J., Zhang G., Lin Y., Li Y. Coupling of thermal mass and natural ventilation in buildings, Energy and Buildings 40 (2008) 979–986.
[14] La Roche P., Milne M., Effects of window size and thermal mass on building comfort using an intelligent ventilation controller, Solar Energy 77 (2004) 421–434.[15] Balaras C.A., The role of thermal mass on the cooling load of buildings. An overview of computational methods, Energy and Buildings 24 (1996) l-10.
[16] Yang L., Li Y., Cooling load reduction by using thermal mass and night ventilation, Energy and Buildings 40 (2008) 2052–2058.
[17] Yam J., Li Y., Zheng Z., Nonlinear coupling between thermal mass and natural ventilation in buildings, International Journal of Heat and Mass Transfer 46 (2003) 1251–1264.
[18] Shaviv E., Yezioro A., Capeluto I.G., Thermal mass and night ventilation as passive cooling design strategy, Renewable Energy 24 (2001) 445–452.
[19] Lee K., Braun J.E., Model-based demand-limiting control of building thermal mass, Building and Environment 43 (2008) 1633–1646.
[20] Braun J.E., Montgomery K.W., Chaturvedi N., Evaluating the Performance of Building Thermal Mass Control Strategies, HVAC&R Research, 7 (2004), 4, 403-428.
[21] Zeng R., Wang X., Di H., Jiang F., Zhang Y., New concepts and approach for developing energy efficient buildings: Ideal specific heat for building internal thermal mass, Energy and Buildings 43 (2011) 1081–1090.

[22] Csáky I., Kalmár F., , Simulation of the internal temperature in the PASSOL Laboratory, University of Debrecen, International Review of Applied Sciences and Engineering, 3, (2012), 63-73.
[23] EN ISO 13790:2008 (2008) Energy performance of buildings – Calculation of energy use for space heating and cooling.
[24] Csáky I., Kalmár F. Effects of thermal mass, ventilation and glazing orientation on indoor air temperature in buildings, Journal of Building Physics 39:(2) pp. 189-204. (2015)
[25] Csáky I., Kalmár F. Effects of solar radiation asymmetry on buildings' cooling energy needs, Journal of Building Physics, 40:(1), (2016), 35-54.
[26] EN15251, (2007), Indoor environmental input parameters for design and assessment of energy performance of buildings addressing indoor air quality, thermal environment, lighting and acoustics, European Committee for Standardization, Brussels.

Highlights

- the effects of thermal mass on the operative temperature was investigated
- the relation between allowable transparent area and thermal mass was analysed
- the relation between thermal mass and air change rate was analysed
- 688 building models were investigated